JOURNAL OF GEOPHYSICAL RESEARCH, VOL. 105, NO. B2, PAGES 2721–2736, FEBRUARY 10, 2000

Record of seamount production and off-axis evolution in the western North Atlantic Ocean, 25°25'-27°10'N

Gary E. Jaroslow
Sea Education Association, Woods Hole, Massachusetts

Deborah K. Smith and Brian E. Tucholke
Department of Geology and Geophysics, Woods Hole Oceanographic Institution, Woods Hole, Massachusetts

Abstract. Using multibeam bathymetry, we identified 86 axial and 1290 off-axis seamounts (near-circular volcanoes with heights ≥ 70 m) in an area of 75,000 km^2 on the western flank of the Mid-Atlantic Ridge (MAR), 25°25'N to 27°10'N, extending ~400 km from the inner rift valley floor to ~29 Ma crust. Our study shows that seamounts are a common morphological feature of the North Atlantic seafloor. Seamount-producing volcanism occurs primarily on the inner rift valley floor, and few, if any, seamounts are formed on the rift valley walls or the ridge flank. The high abundance of off-axis seamounts is consistent with 1-3 km wide sections of oceanic crust being transferred intact from the axial valley to the ridge flank on crust >4 Ma. Significant changes in seamount abundances, sizes, and shapes are attributed to the effects of faulting between ~0.6 and 2 m.y. off axis in the lower rift valley walls. Few seamounts are completely destroyed by (inward facing) faults, and population abundances are similar to those on axis. However, faulting reduces the characteristic height of the seamount population significantly. In the upper portions of the rift valley, on 2-4 Ma crust, crustal aging processes (sedimentation and mass wasting), together with additional outward facing faults, destroy and degrade a significant number of seamounts. Beyond the crest of the rift mountains (>4 Ma crust) faulting is no longer active, and changes in the off-axis seamount population reflect crustal aging processes as well as temporal changes in seamount production that occurred at the ridge axis. Estimates of population density for off-axis seamounts show a positive correlation to crustal thickness inferred from analysis of gravity data, suggesting that increased seamount production accompanies increased magma input at the ridge axis. We find no systematic variations in seamount population density along isochron within individual ridge segments. Possible explanations are that along-axis production of seamounts is uniform or that seamount production is enhanced in some regions (e.g., segment centers), but many seamounts do not meet our counting criteria because they are masked by younger volcanic eruptions and low-relief flows.

1. Introduction

The connection between seamount volcanism and crustal accretion at mid-ocean ridges has been the subject of much discussion. At fast spreading ridges such as the East Pacific Rise (EPR), near-circular submarine volcanoes (seamounts) are found only rarely at the rise axis but are abundant on the rise flanks [e.g., *Searle*, 1983; *Fornari et al.*, 1987; *Batiza et al.*, 1989; *Shen et al.*, 1993; *Scheirer and Macdonald*, 1995; *White et al.*, 1998], and volcanism leading to the formation of seamounts on the flanks of the EPR is thought to be separate from that occurring at the rise axis [e.g., *Scheirer and Macdonald*, 1995]. In contrast, seamounts on the slow spreading Mid-Atlantic Ridge (MAR) are observed both at the axis and on the ridge flanks [e.g., *Litvin and Rudenko*, 1973; *Kong et al.*, 1988; *Batiza et al.*, 1989; *Epp and Smoot*, 1989; *Smith and Cann*, 1990, 1992; *Sempéré et al.*, 1993; *Gente et al.*, 1995]. Most volcano construction is thought to occur at the MAR axis [*Smith and Cann*, 1990, 1992], but very little is known about off-axis volcanism [e.g., *Batiza et al.*, 1989; *Epp and Smoot*, 1989], despite its importance to understanding spatial and temporal supply of magma to the crust during its formation and evolution. Moreover, the processes that modify axial seamounts as they are transported to the ridge flanks are poorly understood, and the resulting abundances, size distributions, and locations of the volcanic edifice remnants have not been quantified.

To obtain a better understanding of the record of on-axis and possible off-axis volcanism at the MAR, we analyzed an extensive multibeam and sidescan sonar data set collected over the western flank of the MAR between 25°25' and 27°10'N, extending from the ridge axis to ~29 Ma crust ~400 km off axis (Figure 1). We quantified seamount population density and seamount shapes within this region to examine (1) the character of seamount production at the MAR axis, (2) the effects of tectonism and crustal aging on the seamount population as crust is transported off axis, (3) the existence of off-axis volcanism, and (4) temporal variations in seamount generation. We also examined the relationship of seamount volcanism to intrasegment tectonic setting and to both intrasegment and regional variation in residual mantle Bouguer anomaly. Finally, because our study area spans several ridge segments, we compared seamount

Paper number 1999JB900253.
0148-0227/00/1999JB900253$09.00

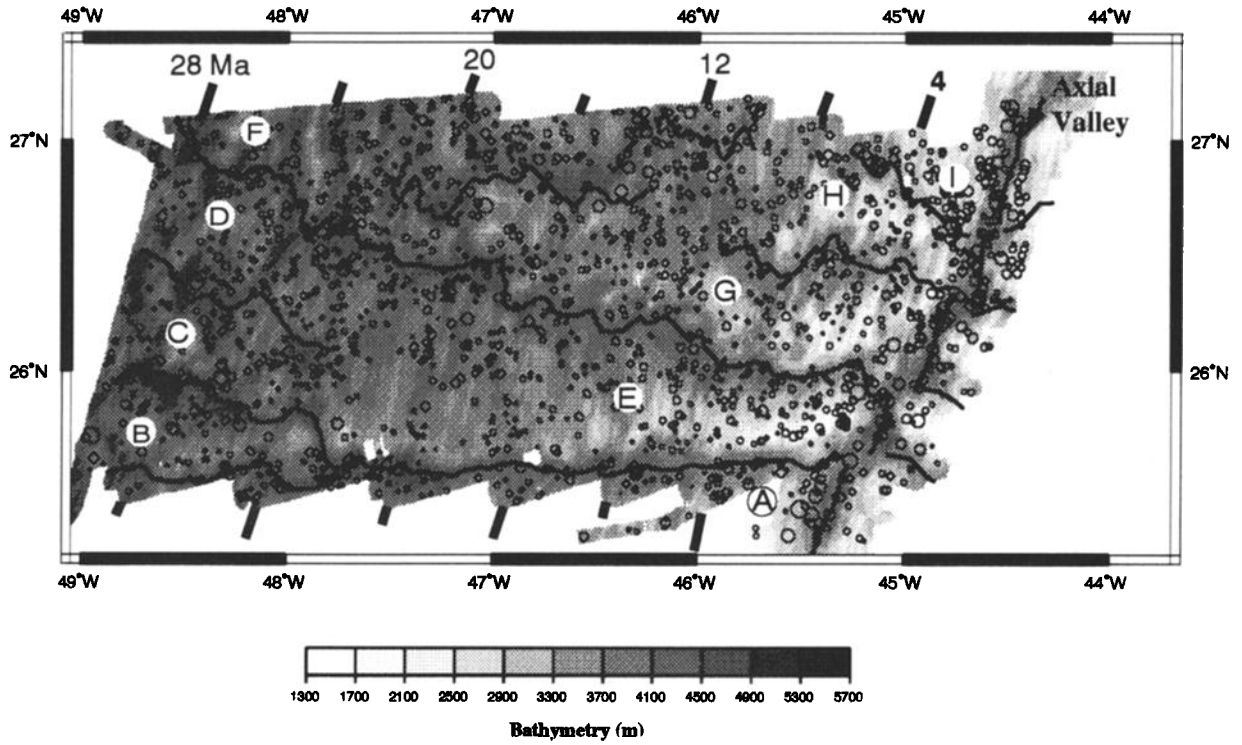

Figure 1. Bathymetric contour map of combined SeaBeam and Hydrosweep multibeam bathymetry. Circles show locations of 1376 identified seamounts with heights ranging between 70 and 560 m; circle size is proportional to mean seamount diameter but is not to map scale. Segment boundaries and the MAR axis, defined by *Tucholke et al.* [1997a], are indicated by thin black lines. Letters denote segment identifications. Crustal ages (Ma) are indicated by numbers and bold lines at edge of survey. Inner rift valley floor contains crust younger than ~ 0.6 Ma.

populations between adjacent segments to determine whether population variations are correlated from segment to segment.

2. Geological Background

The northern Mid-Atlantic Ridge is a slow spreading (≤ 15 mm/yr half-rate) ridge typically marked by a 1.5-3 km deep, 15-30 km wide axial rift valley. The rift valley commonly contains an axial volcanic ridge (AVR) that is several hundred meters high, several kilometers wide, and runs most of the length of individual ridge segments [*Sempéré et al.*, 1993]. The AVR is considered to be the predominant site of volcanic activity within the rift valley [e.g., *Ballard and van Andel*, 1977]. Studies of seamount population density, distribution, and morphology on the rift valley floor [e.g., *Smith and Cann*, 1990, 1992] have led to a general model for eruptions at the MAR [e.g., *Smith et al.*, 1995; *Head et al.*, 1996]. In this model the AVR is formed both by low-relief flows from fissure eruptions and by other volcanic events that produce high relief. If the fissure eruption declines so as to form a number of discrete vents, a hummocky ridge is formed. Rapid evolution of a fissure eruption to a single vent forms a seamount. In an investigation of the seamount population on the inner rift valley floor of the MAR between 24° and 30°N, *Smith and Cann* [1990, 1992] identified >450 seamounts on the AVR summit, flanks, and flanking deeps. Their work demonstrated that seamount volcanism plays a major role in crustal construction.

Ridge segmentation is a fundamental feature of the MAR, and there is an orderly spatial pattern to magmatic and tectonic processes at the segment scale. At the ridge axis, for example, seafloor is shallower and crust is thicker at segment centers than at segment ends [e.g., *Kuo and Forsyth*, 1988; *Lin et al.*, 1990; *Tolstoy et al.*, 1993]. This pattern may be controlled by focusing of mantle upwelling and magmatic accretion near segment midpoints, as has been suggested by geodynamic experiments [*Whitehead et al.*, 1984] and bathymetric and gravity observations [e.g., *Kuo and Forsyth*, 1988; *Lin et al.*, 1990; *Morris and Detrick*, 1991; *Blackman and Forsyth*, 1992]. If so, then intrasegment patterns of construction and distribution of volcanic edifices might reflect this focusing. Studies of cross-isochron variations in residual gravity anomalies also suggest that episodic crustal thickening and thinning occurs with a period of roughly 2-3 m.y. [*Lin et al.*, 1993; *Pariso et al.*, 1995; *Tucholke et al.*, 1997a], and this has been attributed to cyclic variations in melt input from the upwelling asthenosphere. Such temporally variable melt supply might also affect seamount distribution.

As seamounts are transported from the rift valley floor to the ridge flanks, they are likely to be affected by faulting in the rift valley walls. The walls of the MAR rift valley consist of a series of outward tilted fault blocks that are uplifted along inward facing normal faults; along the upper walls the mean topographic gradient is diminished by block rotation and limited extension along outward facing normal faults [*Laughton and Searle*, 1979]. Uplifted fault blocks reach depths as shallow as ~2000 m on 1.5-3.2 Ma crust to form the crest of the rift mountains. Older seafloor is considered to be the "ridge flank," and it progressively deepens with age, roughly following a square root of age relation [cf. *Sclater and Wixon*, 1986]. There is little, if any, faulting beyond the crest of the rift mountains [*Jaroslow*, 1997].

Along-isochron asymmetries in seafloor morphology and

crustal thickness due to segment-scale tectonic variations occur within segments, beginning immediately off axis. Shallow seafloor and exposures of lower crust and upper mantle rocks appear along the inside corners (IC) of spreading segments [*Severinghaus and Macdonald*, 1988; *Tucholke and Lin*, 1994; *Escartín and Lin*, 1995; *Cann et al.*, 1997]. Elevated residual mantle Bouguer (RMBA) gravity values suggest the presence of thin crust at inside corners relative to thick crust at segment centers (SC) and outside corners (OC) [*Tucholke and Lin*, 1994; *Pariso et al.*, 1995; *Tucholke et al.*, 1997a]. IC crustal thinning is thought to be caused by normal-sense, detachment faulting at the ridge axis, with IC crust persistently forming the footwall of the fault [*Dick et al.*, 1981; *Karson*, 1990; *Tucholke and Lin*, 1994; *Cann et al.*, 1997; *Blackman et al.*, 1998]. This asymmetric dissection of young crust might significantly affect the off-axis distribution of seamounts that were created at the ridge axis.

The off-axis population of seamounts on the MAR has been little studied and is poorly understood. A study of classified U.S. Navy bathymetry by *Epp and Smoot* [1989] suggested that no seamounts with relief greater than ~100 m would be found off axis in the North Atlantic south of ~30°N. A study of the rift valley and ridge flanks in the South Atlantic at 26°S by *Batiza et al.* [1989] documented 50 off-axis seamounts with heights ≥50 m on ~1-7 Ma crust and 38 seamounts on crust younger than ~1 Ma. *Batiza et al.* noted that the observed spatial density of the seamount population (i.e., the number of seamounts per unit area) decreases with increasing seafloor age, suggesting either that seamounts are destroyed or buried during transport out of the rift valley, or that the rate of seamount production on the rift valley floor has varied with time. They also noted that relatively fresh lavas were dredged from some off-axis seamounts, and they interpreted this to mean that the ridge-flank seamounts probably were formed outside the rift valley.

3. Study Area

The study area is located north of the Kane Fracture Zone between 25°25' and 27°10'N and extends ~400 km west from the ridge axis to 29 Ma crust (Figure 1). The regional rift valley geology has been reviewed by *Sempéré et al.* [1993], and the ridge axis and ridge flank geology is also discussed by *Tucholke et al.* [1997a].

Our study encompasses nine current and former spreading segments (segments A-I, Figure 1). Segments A, E, G, H and I are currently active segments with well-defined rift valleys having relief of ~2500-2700 m. The inner rift valley floor in each of these segments averages 7 km in width and generally is delineated by opposing, inward facing bounding faults that have throws of 200 m or more. The rift valley floor of segment G at 26°08'N includes the trans-Atlantic geotraverse (TAG) hydrothermal field, which has been the focus of intense geological and geophysical study [e.g., *Rona et al.*, 1976; *Temple et al.*, 1979; *Karson and Rona*, 1990; *Kleinrock and Humphris*, 1996].

Off axis the limits of ridge segments are defined mostly by nontransform discontinuities with age offsets <1-2 m.y. (<30 km), although offset locally reaches 3 m.y. (58 km). Discontinuities are marked by both offsets in magnetic anomalies and relatively deep seafloor, and they rarely show ridge-normal seafloor structure. They are predominantly right-stepping, but north of segment D they also have had short-lived left-stepping or zero offsets [*Tucholke et al.*, 1997a]. About 24-22 Ma a marked counterclockwise change in relative plate motion occurred, rotating the prevailing orientation of abyssal hills, faults, and magnetic anomalies from 024°-015°. Several changes in plate boundary segmentation accompanied the rotation [*Tucholke et al.*, 1997a]. Segments C and D combined to form segment E, and segment F split into segments G and H. Segment B subsequently died out by 19 Ma. Segments E, G, and H have persisted to the present. The along-isochron lengths of these segments vary from ~35 to 100 km and have changed in response to along-axis migration of the intervening discontinuities; segment E has steadily shrunk to its present length of ~35 km.

Sediment cover is highly variable across the area, but nowhere averages more than ~50 m thick, as determined from seismic reflection profiles [*Jaroslow*, 1997]. Sediment thicknesses averaged in 1 m.y. bins along isochrons increase to a maximum of 50 m on ~17 Ma crust and decrease to ~25 m on 28 Ma crust. Locally, thick sediments are ponded in crustal depressions, notably in the deep discontinuities between segments (~200-800 m) and in ridge-parallel valleys between abyssal hills (~50-350 m). Elevated basement between these isolated ponds rarely has sediments thicker than ~10-20 m.

4. Data and Methods

We combined two multibeam bathymetric data sets to obtain nearly 100% bathymetric coverage of an ~75,000 km^2 area of the MAR and its western flank (Figure 1). SeaBeam bathymetry data of *Purdy et al.* [1990] cover the rift valley and the rift mountains to ~30 km off axis. Hydrosweep bathymetry collected during *Ewing* cruise 9208 [*Tucholke et al.*, 1992] provided off-axis coverage westward to 26-29 Ma crust. Both data sets were gridded at 200 m intervals using similar gridding and contouring algorithms.

Seamounts were identified in 20 m contour bathymetric maps as circular to subcircular topographic highs with plan view aspect ratios of <2, following *Smith and Cann*'s [1990, 1992] criteria for seamount identification. An example of this identification is shown in Figure 2. *Smith and Cann* [1990, 1992] identified features on the inner rift valley floor with relief >50 m as seamounts. We increased this minimum height to 70 m so as to identify seamounts more confidently in the faulted, irregularly sedimented terrain of the rift mountains and the ridge flank.

For each seamount we recorded latitude, longitude, and minimum depth of the seamount top and latitude, longitude, and water depth of the end points of the minimum and maximum plan view shape axes. The shape parameters derived from these measurements are D_{min}, the minimum basal diameter; D_{max}, the maximum basal diameter; D_{max}/D_{min}; the aspect ratio (elongation); ϕ, the strike of D_{max}; D_b, the average of the measured basal diameters; z_b, the average basal water depth, taken as the average of the four basal depths recorded; h, seamount height, the difference between z_b and summit depth; and ξ_d, the height-to-diameter ratio of height divided by average basal diameter.

We use the methodology of *Jordan et al.* [1983] and *Smith and Jordan* [1988] to characterize and objectively compare the spatial density (number of seamounts per unit area) and characteristic size of seamount populations. These studies examined several models for seamount size distribution and considered that the exponential model was a good approximation for the distribution (see *Jordan et al.* [1983] and *Smith and Jordan* [1988] for detailed discussion). Following these studies, we assume that the seamount size distribution is nearly exponential over a large range in heights. That is, the average number of seamounts with summit height $h \geq H$ has the expected value

$$\nu(H) = \nu_0 e^{-\beta H},$$

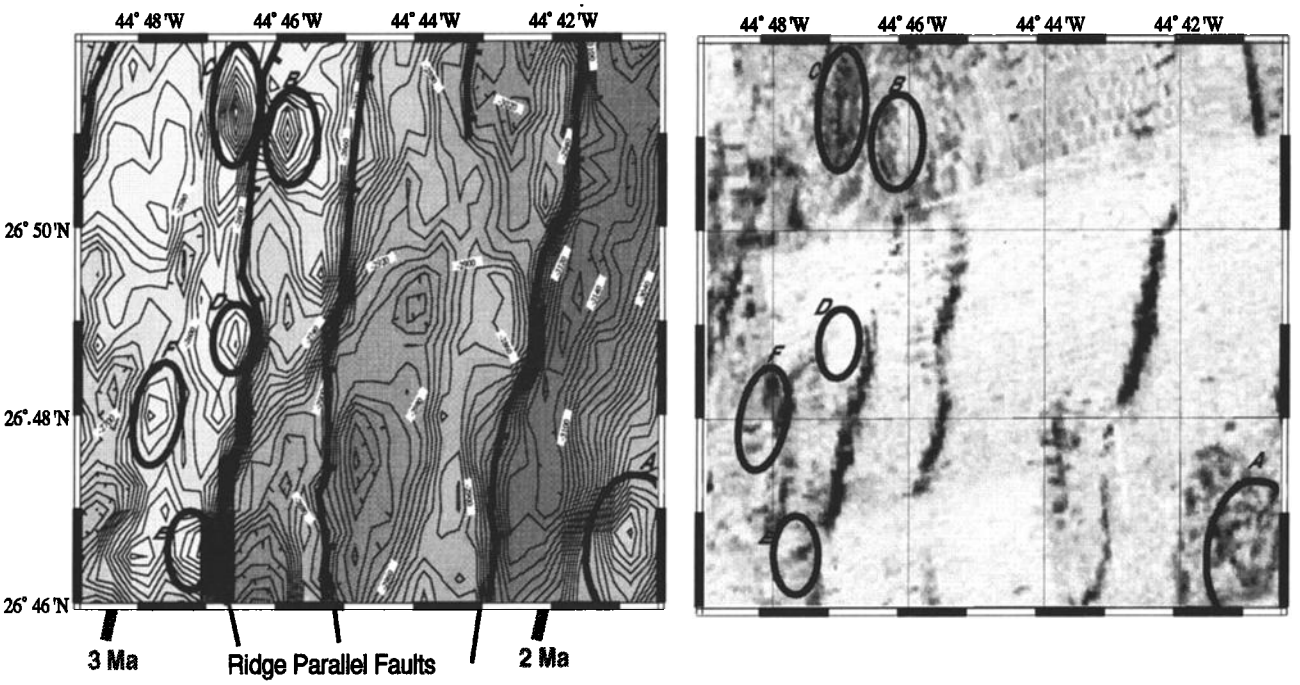

Figure 2. (left) Seamount picks (ovals) identified in bathymetry of ~2-3 Ma seafloor contoured at 20 m interval. Inward and outward facing ridge-parallel faults are shown by thick lines with ticks on the down faulted block. Crustal ages are indicated at gray lines. (right) NNW looking HMR1 sidescan sonar image of same region with seamounts indicated.

where ν_o is the average number of seamounts of all sizes per unit area and β^{-1} is the characteristic height of the population. For this analysis we sorted seamounts into height bins of 25 m, starting with a minimum height of 70 m. Seamount populations in our study area are well characterized by the exponential model and can be described by the two parameters ν_o and β^{-1}. In the following discussion, instead of presenting ν_o, the expected number per unit area, we use ν_α ("population density"), the expected number per 10^3 km^2 ($\nu_\alpha = \nu_o \times 10^9$). Uncertainties in the parameters are given as one standard deviation. In some instances, we also evaluated seamount population density as "observed population density," n/A (number per 10^3 km^2); this was done where the seamount counts were too small to provide a statistically significant value for ν_α (e.g., for small age bins within individual segments).

To investigate temporal changes in the population and shape parameters, seamounts were assigned the same age as the underlying crust, as dated from magnetic anomalies [*Tucholke et al.*, 1997a]. Seamounts located on the inner rift valley floor are referred to as axial seamounts and have ages less than or equal to ~0.6 Ma; those located outside the inner rift valley floor are considered to be off-axis seamounts and range in age from ~0.6-29 Ma. We divided the off axis population into eight age bins as follows: 0.6-2 Ma, seamounts located off axis and generally on the lower walls of the rift valley; 2-4 Ma, seamounts on the upper walls of the rift valley and along the crest of the rift mountains; and six 4 m.y. intervals out to 28 Ma on the ridge flank. The age range of bins off axis was selected so as to be large enough to provide a statistically robust sample in each bin and yet small enough to highlight details of age-related variations in popula-

Table 1. Seamount Population Characteristics Sorted by Crustal Age

Age, Ma	Number of Seamounts	Area, 10^3 km^2	Characteristic Height β^{-1}, m	Population, Density ν_{ot}, number per 10^3 km^2	Height to Diameter Ratio ξ_d	Elongation D_{max}/D_{min}
0-0.6 (axial)	86	2.8	91.5 ± 3.7	75.9 ± 8.5	0.09 ± 0.02	1.3 ± 0.2
0.6-28 (off axis)	1290	70.7	51.2 ± 1.2	58.3 ± 1.6	0.13 ± 0.04	1.4 ± 0.3
0.6-2	85	2.8	69.2 ± 3.7	74.6 ± 8.4	0.09 ± 0.02	1.4 ± 0.3
2-4	97	4.1	70.1 ± 3.4	58.5 ± 6.2	0.13 ± 0.06	1.4 ± 0.3
4-8	178	8.5	74.1 ± 2.5	52.2 ± 4.0	0.13 ± 0.04	1.4 ± 0.3
8-12	179	10.4	69.1 ± 2.9	42.2 ± 3.2	0.14 ± 0.05	1.5 ± 0.3
12-16	182	11.8	61.2 ± 2.8	41.5 ± 3.1	0.13 ± 0.04	1.4 ± 0.3
16-20	207	11.8	56.8 ± 2.2	52.7 ± 3.8	0.12 ± 0.04	1.5 ± 0.2
20-24	200	9.9	52.1 ± 2.6	65.4 ± 4.7	0.13 ± 0.04	1.5 ± 0.3
24-28	162	11.5	51.1 ± 2.5	47.2 ± 3.8	0.13 ± 0.04	1.5 ± 0.3

tion, especially near the ridge axis where faults are active (Table 1).

Hawaii MR1 (HMR1) long-range sidescan sonar images of the seafloor were used to evaluate the ages of seamounts relative to adjacent seafloor. The HMR1 data [*Tucholke et al.*, 1992] provide 100% seafloor coverage in both NNW and SSE look directions. We first studied the backscatter from off-axis seamounts for indications of young lava flows. At mid-ocean ridges the rain of pelagic sediment produces an almost linear decay in average backscatter strength away from the ridge axis, and regions of high backscatter represent surfaces where sediment does not significantly attenuate the backscatter signal [*Mitchell*, 1993]. Our analysis showed that no off-axis seamounts have high backscatter relative to surrounding seafloor, suggesting that they are approximately the same age as the crust on which they were built.

We also examined the sidescan sonar imagery for geological relations between faults and seamounts (e.g., Figure 2). Dissection of a seamount by faults indicates that the seamount was formed prior to faulting, i.e., prior to exiting the rift valley. Growth of a seamount's volcanic apron over a fault would indicate that the seamount postdates the fault and thus would have been formed on crust beyond the inner rift valley bounding fault. We found no evidence of seamounts being constructed across preexisting faults, although many seamounts are crosscut by faults. We conclude from these observations that the seamounts studied here were constructed on the inner rift valley floor and that off-axis volcanism is not important in our study area.

From detailed mapping of sediment thickness [*Jaroslow*, 1997] we recognize that there are areas where sediment thickness is ≥70 m, the minimum height of seamounts analyzed in this study. Smaller seamounts may be wholly or partially buried by sediments. Thus our estimates of $\nu_{\alpha t}$ are considered to be minimum values. However, partial burial of a population of similar age seamounts does not change the characteristic height of the population because all individual seamount heights are uniformly affected, and the distribution of seamount heights would remain the same.

5. Seamount Population Comparisons

5.1. Axial Versus Off-Axis Seamount Populations

We identified 86 axial and 1290 off-axis seamounts with heights ranging from 70 to 560 m (Figure 1 and Table 1). Average slopes on the seamount flanks range from 10° to 16°. There are many seamount-like topographic highs in the off-axis bathymetry that have heights ≥70 m but have plan view shapes that form only a portion of a circle and whose aspect ratio is >2. Many of these may be seamounts that have been dissected by faults; however, by our identification criteria, these are not identified as seamounts, and hence they are excluded from our study.

Population characteristics of axial and off-axis seamounts differ significantly from one another (Table 1). Numbers of seamounts versus seamount heights h are plotted in Figure 3 for these populations, together with the best fitting exponential model in Figures 3c and 3d. The characteristic height of the axial seamounts is estimated as $\beta^{-1} = 92 \pm 4$ m, which is significantly higher than that of the off-axis population at $\beta^{-1} = 51 \pm 1$ m. Likewise, the axial seamount population density is signifi-

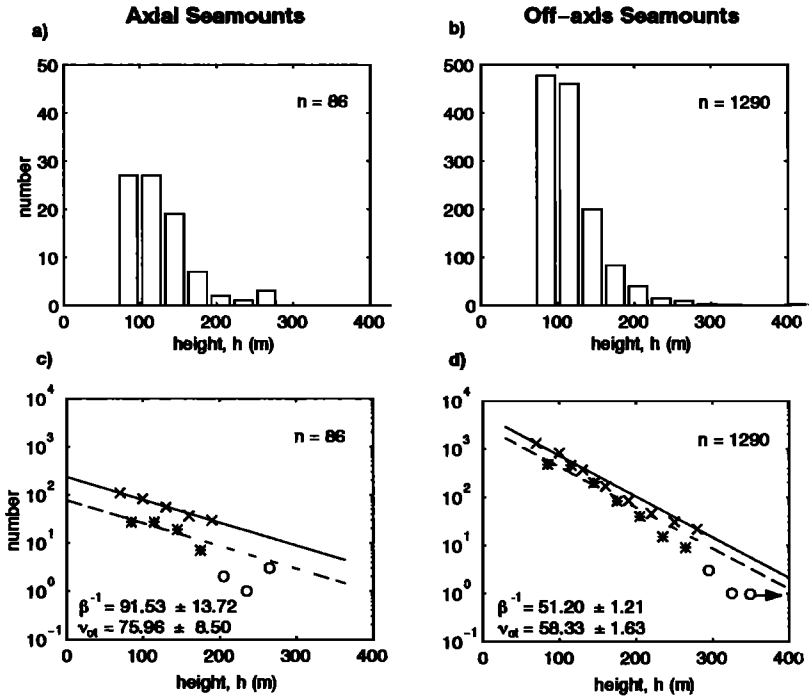

Figure 3. (a and b) Binned height distributions of axial and off-axis seamounts ≥70 m high. (c and d) Number of axial and off-axis seamounts versus seamount height. Stars are binned counts in 25 m height bins; Crosses are cumulative counts. Open circle data are not included in the statistical analyses because of small numbers of seamounts at these heights. Maximum likelihood fits to the data show that the distributions can be modeled with exponential size-frequency curves (solid line is fit of cumulative data; dashed line is binned data). Line slope is the characteristic height of the seamount population β^{-1} and the line intercept at zero height, when normalized to area, defines the population density ν_{α}

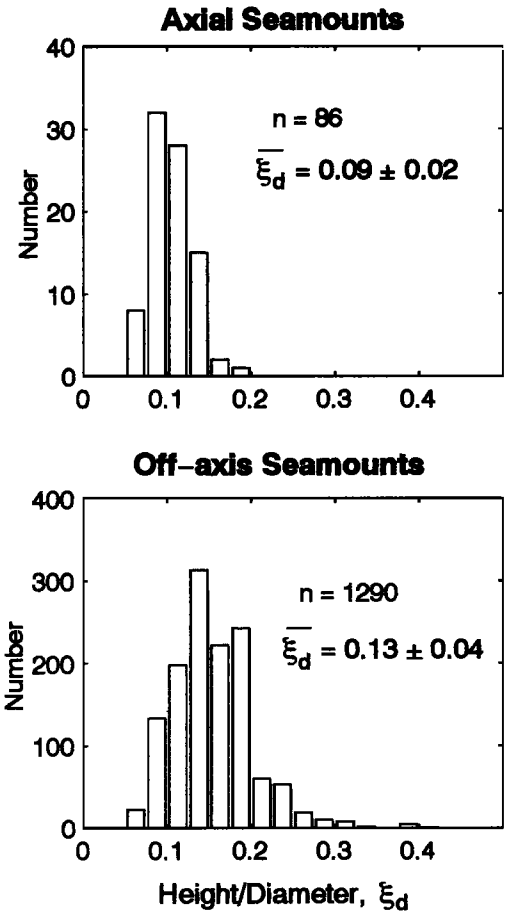

Figure 4. Histograms of the seamount height-to-diameter ratio ξ_d for all axial and off-axis seamounts. Bin size is 0.025. Off-axis seamounts have ratios that span a larger range, and the distribution of values is shifted to a higher average ξ_d compared to the axial seamounts. This indicates that off-axis seamounts have smaller diameters than their axial counterparts with similar heights.

cantly greater, with ν_α = 76 ± 8 per 10^3 km^2 compared to 58 ± 2 per 10^3 km^2 for off-axis seamounts.

Shapes of seamounts, characterized by basal diameter D_b and height-to-diameter ratio ξ_d also show marked differences between the axial and off-axis populations. The basal diameter of axial seamounts ranges from 700 to 2650 m, which is a narrower range than that of off-axis seamounts, which range from 275 to 3125 m. The mean height-to-diameter ratio of seamounts increases from ξ_d = 0.09 ± 0.02 on axis to ξ_d = 0.13 ± 0.04 off axis (Figure 4).

Orientations of axial seamounts ϕ vary widely and do not show a strong trend, whereas off-axis seamounts show distinct orientation patterns (Figure 5). Off-axis seamounts of age 0.6-22 Ma have orientations concentrated at ~355°-020°, and older seamounts of age 22-28 Ma have orientations of ~000°-035°. The counterclockwise shift in ϕ ~22 Ma matches a marked counterclockwise change in spreading direction from ~114° to ~105° at that time [*Tucholke et al.*, 1997a].

5.2. Temporal Variations in Seamount Population

Our study of backscatter from seamounts in HMR1 sidescan data and the observed geological relations between seamounts and faults suggest that all seamounts in this region are formed at the ridge axis (on crust <0.6 Ma). Using this assumption, we measured cross-isochron variations in seamount populations to examine (1) how seamounts are modified during tectonic transport from the inner rift valley floor to the ridge flank, (2) the effects of seafloor aging processes, and (3) temporal changes in axial seamount production.

The decrease in population density of seamounts from on to off axis does not occur immediately as crust is transported beyond the inner rift valley bounding faults; on crust 0.6-2 Ma the population density is approximately the same as that on the inner rift valley floor (Figure 6a). It is only in the upper rift valley walls and on the ridge flank on crust older than 2 Ma that population density significantly decreases. Population density decreases steadily on crust older than 2 Ma, reaching a minimum on crust of age 8-16 Ma. It then increases on crust of age 16-24 Ma, peaking in the 20-24 Ma range, before again decreasing on older crust.

The characteristic height of seamounts also changes over time (Figure 6b), decreasing from the axial maximum of β^{-1} = 92 ± 4 m. Unlike seamount population density, a dramatic decrease in β^{-1} occurs immediately off axis in the lower rift valley walls on

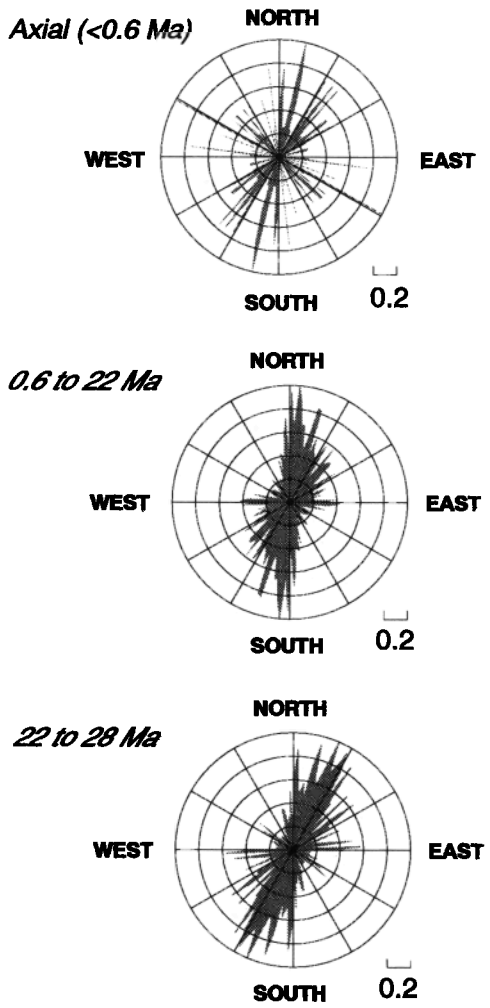

Figure 5. Rose diagrams showing the strike of seamount orientation, as determined by seamount D_{max} (long axis) for three age groupings. Frequency distributions are normalized to 1, with circles indicating 0.2 fractional increments.

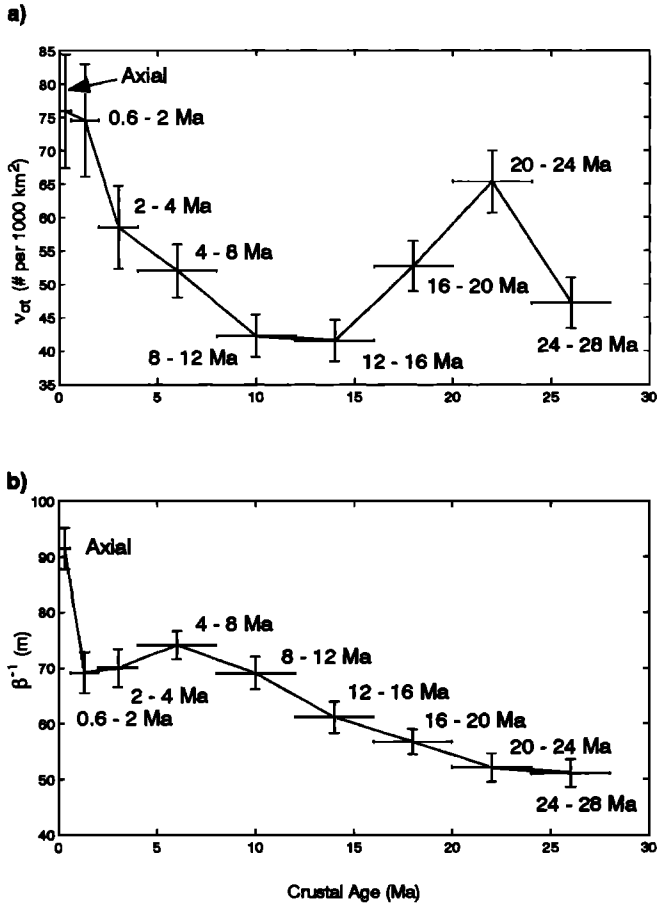

Figure 6. Seamount population parameters plotted versus crustal age. (a) Expected number of seamounts of all sizes per 10^3 km^2, ν_{α} (b) Characteristic height of the seamount population β^{-1}. Ranges of age bins and errors of one standard deviation are shown by bars. Values of the parameters and their errors are given in Table 1. Seamount population density does not decrease from the axial region (<0.6 Ma) to the lower rift valley walls (0.6-2 Ma), but characteristic height decreases significantly.

crust 0.6-2 Ma (β^{-1} = 69 ± 4 m). At greater ages the seamount populations show an overall, progressive decrease in characteristic height, with only slight increase at the 4-8 Ma range.

To examine trends in seamount shape over time, we plot the running means of height-to-diameter ratio ξ_d against seamount height h for all age bins (Figure 7). We distinguish between 2-3 Ma and 3-4 Ma seamounts to gain insight into near-axis changes. Data for the more statistically robust 2 to 4 Ma age bin are given in Table 1. Axial seamounts and those in the lower rift valley walls (0.6-2 Ma) have significantly lower height-to-diameter ratios than seamounts located on crust >3 Ma. Because the off-axis populations also have smaller characteristic heights, it appears that the diameters of axial seamounts are being significantly reduced when they exit the rift valley. In addition, axial seamounts have ξ_d that is approximately constant over the entire height range, whereas off-axis seamounts shift to higher values of ξ_d following larger heights. Thus large (tall) seamounts in the off-axis population are the seamounts most likely to be modified.

We used population parameters estimated for segments C, D, and E (Figure 1) to investigate changes that may have been associated with the plate motion change that occurred ~24-22 Ma. Segments C and D evolved into segment E at the time of the plate motion change, and as a group these segments constitute the longest contiguous crustal record between mapped discontinuities within the survey area. Seamount population densities are similar in segments C (ν_{α} = 80.9 ± 9.8) and D (ν_{α} = 85.9 ± 7.9) (Table 2), but these values are significantly greater than population density in the ensuing segment E (ν_{α} = 64.6 ± 3.8). Characteristic heights are quite different between segments D (β^{-1} = 54.9 ± 2.8) and C (β^{-1} = 44.9 ± 2.8), with intermediate heights in segment E (β^{-1} = 50.8 ± 2.3). These observations suggest reduced seamount production at the time of the plate motion change, accompanied by formation of a population with heights intermediate between the extremes observed in the preceding segments C and D.

5.3. Variations in Seamount Population Between Segments

Seamount population parameters for individual segments are compared in Table 2. Only segments that contain >60 seamounts and that are bounded on both ends by discontinuities (Figure 1) are included in this comparison. Comparison of seamount populations in segments E, G, and H shows significant northward trends of both increasing seamount population density and increasing characteristic height from segment to segment. An even more pronounced northward increase in population density is observed for the older segments B, C, and D but with no comparable increase in characteristic height.

We also compared one segment to another in terms of population density versus crustal age. There are no significant correlations observed, so seamount populations appear to have developed independently from one segment to another.

5.4. Seamount Population Variations Correlated With Gravity

To assess possible relationships between seamount production and inferred crustal thickness, we compared seamount parameters against residual mantle Bouguer anomaly. RMBA is calculated by removing the gravity effects of seafloor topography, a constant thickness crust, and the thermal effects of lithospheric cooling [*Kuo and Forsyth*, 1988; *Lin et al.*, 1990; *Lin and Phipps Morgan*, 1992]. Residual gravity lows are interpreted to represent regions of thicker crust and/or hotter, low-density upper mantle compared to regions of residual gravity highs. Thus residual gravity lows are expected to be in regions of elevated melt accumulation.

To compare seamount populations to variations in RMBA, we divided residual gravity values over the study area into three ranges: low (< 7 mGal), intermediate (7-15 mGal), and high (> 15 mGal). Figure 8 shows the resulting gravity anomaly pattern together with locations of seamounts. Individual spreading segments have broadly different RMBA signatures. Segment E exhibits low residual gravity, suggesting that its crust is relatively thick. In contrast, Segment G has more elevated residual gravity, indicating thinner crust. Segment H contains a mixed pattern of residual gravity highs and lows. Within each segment, IC settings tend to be marked by residual gravity highs (thin crust), while segment centers and outside corners correspond to regions of low and intermediate gravity (thick and intermediate crust), respectively [*Tucholke et al.*, 1997a]. Across isochrons, residual gravity anomalies fluctuate by 10-20 mGal with a period of ~2-3 Ma, suggesting cyclic changes of at least 1-2 km in crustal thickness [*Lin et al.*, 1993; *Tucholke et al.*, 1997a].

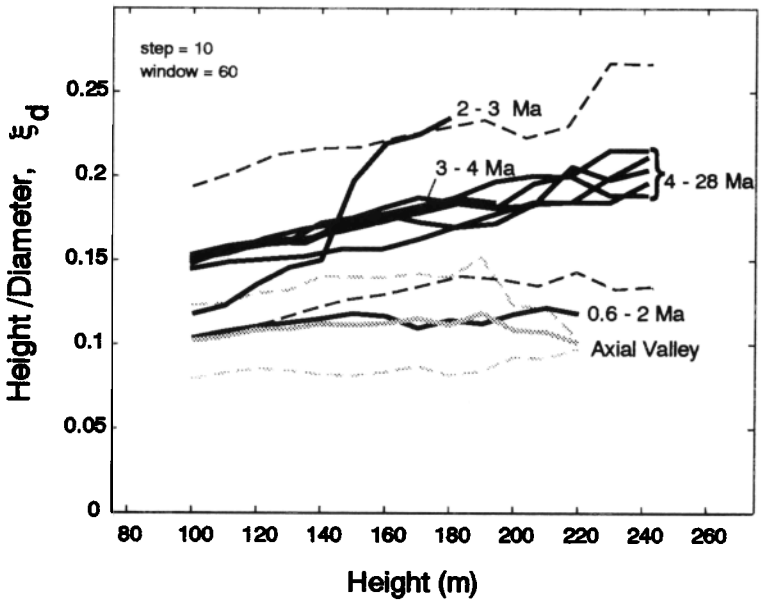

Figure 7. Running mean of height-to-diameter ratio ξ_d versus height for seamount populations sorted by crustal age. Dashed lines indicate maximum bound of one standard deviation errors for axial (0-0.6 Ma; stippled lines) and off-axis (2-28 Ma; solid lines) seamounts. Running means were derived using height step sizes of 10 m and ranges of 60 m. Note that ξ_d increases on crust >3 Ma.

Seamount population parameters for the three ranges of RMBA are listed in Table 3. Estimated population density in regions of low to intermediate residual gravity is significantly greater than that in regions of residual gravity highs; that is, seamounts occur more frequently on inferred thicker crust. The characteristic heights are similar for all gravity ranges.

We observe no significant correlation between cross-isochron values of the observed number of seamounts per area *n/A* and residual gravity, but the mean RMBA used in each age bin incorporates strong along-isochron variations (Figure 8). Thus lack of cross-isochron correlation between *n/A* and residual gravity may not be meaningful.

Finally, we found no significant associations between RMBA variations in adjoining segments. Although our along-isochron averaging of RMBA values may mask real correlations, the result is like that of a similar, negative finding along the MAR near the Atlantis Fracture Zone [*Pariso et al.*, 1995].

5.5. Variations in Seamount Population With Tectonic Setting

We subdivided data on seamount population density and characteristic height along isochrons within each segment to examine possible variations related to IC, SC, and OC tectonic setting. We examined only segments where both segment ends are defined by identified discontinuities (segments B, C, D, E, G and H; Figure 1). To compare intrasegment variations objectively, each of the IC, SC, and OC settings was defined as one third of the along-isochron distance between discontinuities bounding a segment. This method was chosen to highlight along-isochron differences in seamount population that might be related to three-dimensional magmatic upwelling at the centers of segments. We also used a second method, wherein IC crust was defined as 14% of the along-isochron distance from the boundary at the IC edge of the segment. This reflects the approximate average limit of irregular, arcuate, and oblique faults that are typical of IC crust [*Jaroslow*, 1997]. Outside corner crust was defined as 30% of segment length from the OC edge, and the remainder of the length was considered to be SC crust. This method allows for better examination of possible correlations between seamount population and real intrasegment variations in tectonic pattern. Where discontinuity offset was zero and the segment boundary was thus poorly defined, crust was assigned to the same tectonic setting as that of younger crust in the segment, where the discontinuity is well known.

Table 2. Seamount Population Characteristics for Individual Segments

Segment *	Number of Seamounts	Area, 10^3 km^2	Characteristic Height β^{-1}, m	Population Density, ν_{ot}, number per 10^3 km^2
B	60	4.2	59.8 ± 4.8	50.7 ± 6.6
C	74	4.6	44.9 ± 2.9	80.9 ± 9.8
D	124	5.6	54.9 ± 2.8	85.9 ± 7.9
E	292	18.5	50.8 ± 2.3	64.6 ± 3.8
G	228	11.2	57.8 ± 2.1	74.5 ± 5.1
H	245	9.2	68.4 ± 2.5	80.4 ± 5.2

* Segments move from south to north from B to D and from E to H.

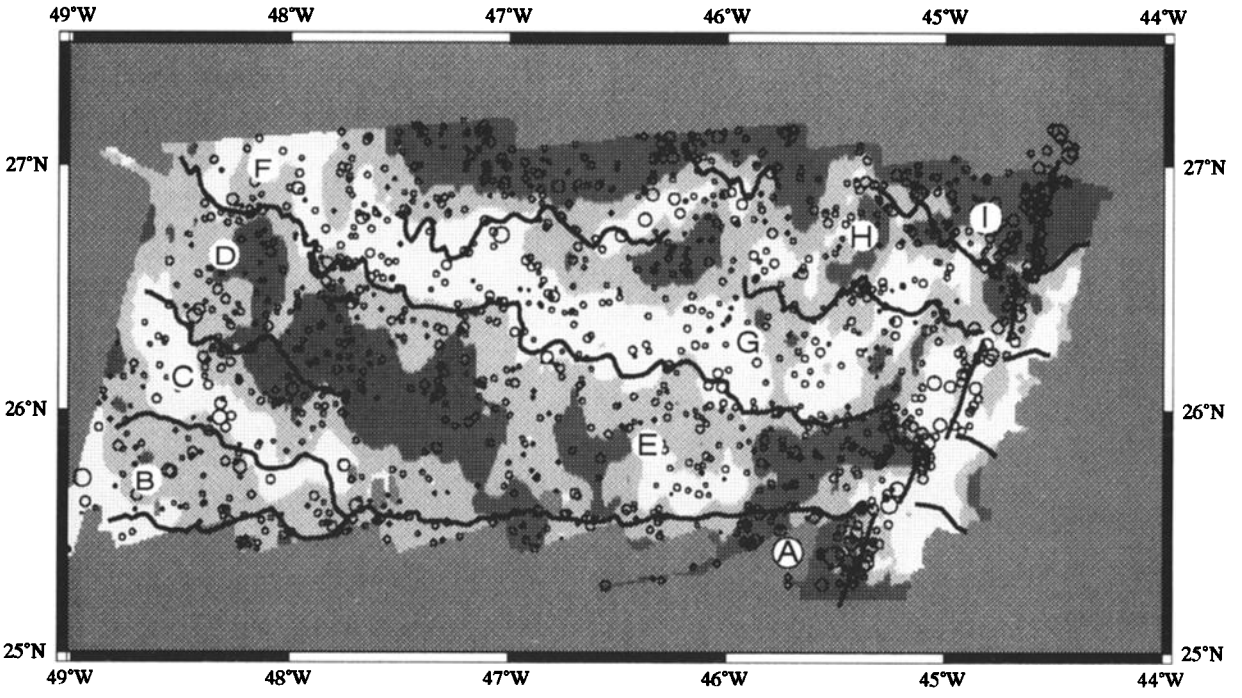

Figure 8. Map of residual mantle Bouguer gravity anomaly (RMBA) [*Tucholke et al.*, 1997a] with seamount locations (circles) superimposed. Shading shows RMBA gravity <7 mGal (dark gray), 7-15 mGal (medium gray), and >15 mGal (light gray). Segment boundaries are as in Figure 1. Associated seamount population characteristics are listed in Table 3 and show that seamount population density is positively correlated with crustal thickness inferred from the gravity data.

Population characteristics in relation to along-isochron position for these two sorting methods are given in Table 4. Considering the correlation noted earlier between RMBA and population density and because IC are generally marked by elevated RMBA compared to the remaining portions of segments, we expect that seamount population density at IC would be reduced. A possible explanation is that seamount characteristic heights and expected population densities show no major changes with respect to intrasegment tectonic setting under either sorting method. However, RMBA values within a given tectonic setting change significantly both from segment to segment and across isochrons within a segment, and averaging the RMBA values within a tectonic setting may mask any correlation between seamount population density and IC tectonic setting.

6. Discussion

Our identification of 86 axial and 1290 off-axis seamounts on the western flank of the MAR shows that seamounts are common features on the North Atlantic seafloor. Our analyses indicate that the seamounts are produced primarily on the inner rift valley floor and that few, if any, seamounts are formed within the rift valley walls or on the ridge flank. This interpretation is based on the following observations. (1) Seamounts are a ubiquitous volcanic product on the inner rift valley floor of the MAR between 24° and 30°N [e.g., *Smith and Cann*, 1990; 1992]. (2) Sidescan sonar images show that backscatter from off-axis seamounts is not elevated in relation to backscatter from comparable slopes on adjacent seafloor, suggesting that the seamounts have ages similar to the crust on which they reside. (3) There is no bathymetric or sidescan sonar evidence for growth of seamount volcanic aprons across preexisting fault scarps. (4) Faults commonly cut the off-axis seamounts. (5) Off-axis seamount population density is consistently lower than that of axial seamounts. Assuming that observed off-axis seamounts were formed on the inner rift valley floor, changes in seamount parameters with age must reflect the effects of faulting as seamounts are transported out of the rift valley, the effects of seafloor aging (sedimentation and mass wasting), and temporal variations in axial seamount production.

Table 3. Off-Axis Seamount Population Characteristics in Relation to Residual Mantle Bouguer Anomaly (RMBA)

RMBA, mgal	Number of Seamounts	Area, 10^3 km^2	Characteristic Height β^{-1}, m	Population Density ν_{ot}, number per 10^3 km^2
Low (<7)	472	22.9	58.3 ± 1.9	70.7 ± 3.3
Medium (7-15)	595	32.1	55.1 ± 1.5	69.6 ± 2.9
High (>15)	298	20.5	61.4 ± 1.9	50.2 ± 3.0

Table 4. Seamount Population Characteristics in Relation to Along-Isochron Position

Province		Number of Seamounts	Area, 10^3 km^2	Characteristic Height β^{-1}, m	Population Density ν_{ot}, number per 10^3 km^2
Inside Corner	(33%)	352	18.0	56.5 ± 1.7	73.4 ± 4.0
Segment Center	(33%)	362	18.0	58.1 ± 2.0	71.4 ± 3.8
Outside Corner	(34%)	355	18.6	56.3 ± 2.2	68.0 ± 3.7
Inside Corner	(14%)	167	9.5	52.8 ± 2.4	71.1 ± 5.6
Segment Center	(56%)	588	28.7	56.4 ± 1.5	74.8 ± 3.1
Outside Corner	(30%)	313	16.4	55.7 ± 2.4	68.6 ± 3.9

6.1. Modification of Seamounts During Transport Off Axis

The preservation of large numbers of off-axis seamounts that originated on the inner rift valley floor provides compelling evidence that rift valley faults are spaced widely enough that seamounts are commonly transported off axis without being destroyed (Figure 9). Nonetheless, off-axis changes in seamount population density, size, and shape suggest that faulting and aging processes do destroy some seamounts and strongly modify others. These changes are concentrated in the rift valley walls on 0.6-4 Ma crust (Figures 6, 7), and we show them in expanded form in Figure 10. At the top of Figure 10 is a conceptual cross section of the ocean crust that highlights fault patterns consistent with a separate fault analysis of the study area [G. Jaroslow and B. E. Tucholke, manuscript in preparation, 1999] and with our seamount observations.

6.1.1. Axial Seamounts. Where seamounts are generated on the inner rift valley floor (zone 1, Figure 10), faults are discontinuous and have small throws of typically < 50 m. Population and shape parameters of these axial seamounts therefore are little affected by faulting. Instead, other variables most likely control the axial population density, including the amount of magma delivered to the crust, its ability to erupt, and the style of emplacement (low-relief flow versus edifice construction) [e.g., *Ballard et al.*, 1979; *Bonatti and Harrison*, 1988]. Similarly, the height to which a seamount builds depends on several variables, most important of which must be magma volume and pressure within the magma reservoir [*Head et al.*, 1996].

As throughout the study region, plan view shapes of seamounts on the inner rift valley floor have elongations (D_{max}/D_{min}) that range between 1 (circular) and 2 (elliptical, the upper limit of our identification criterion). The elongate shapes

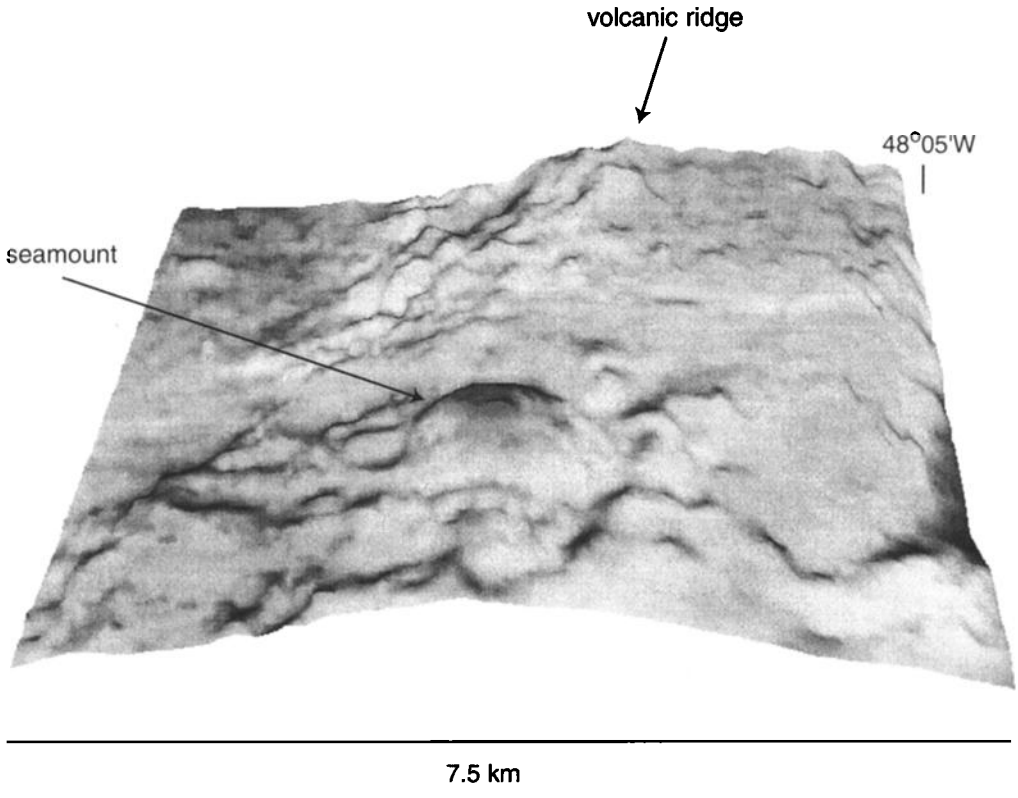

Figure 9. Shaded, three-dimensional bathymetry of a fossil axial volcanic ridge (25 Ma) that has been transported intact onto the ridge flank. Seamount height and diameter are ~250 m and 2 km, respectively. Observations of intact seamounts and volcanic ridges on the flanks of the MAR suggests that in places, large sections of the oceanic crust move to the flanks without being disrupted by faults.

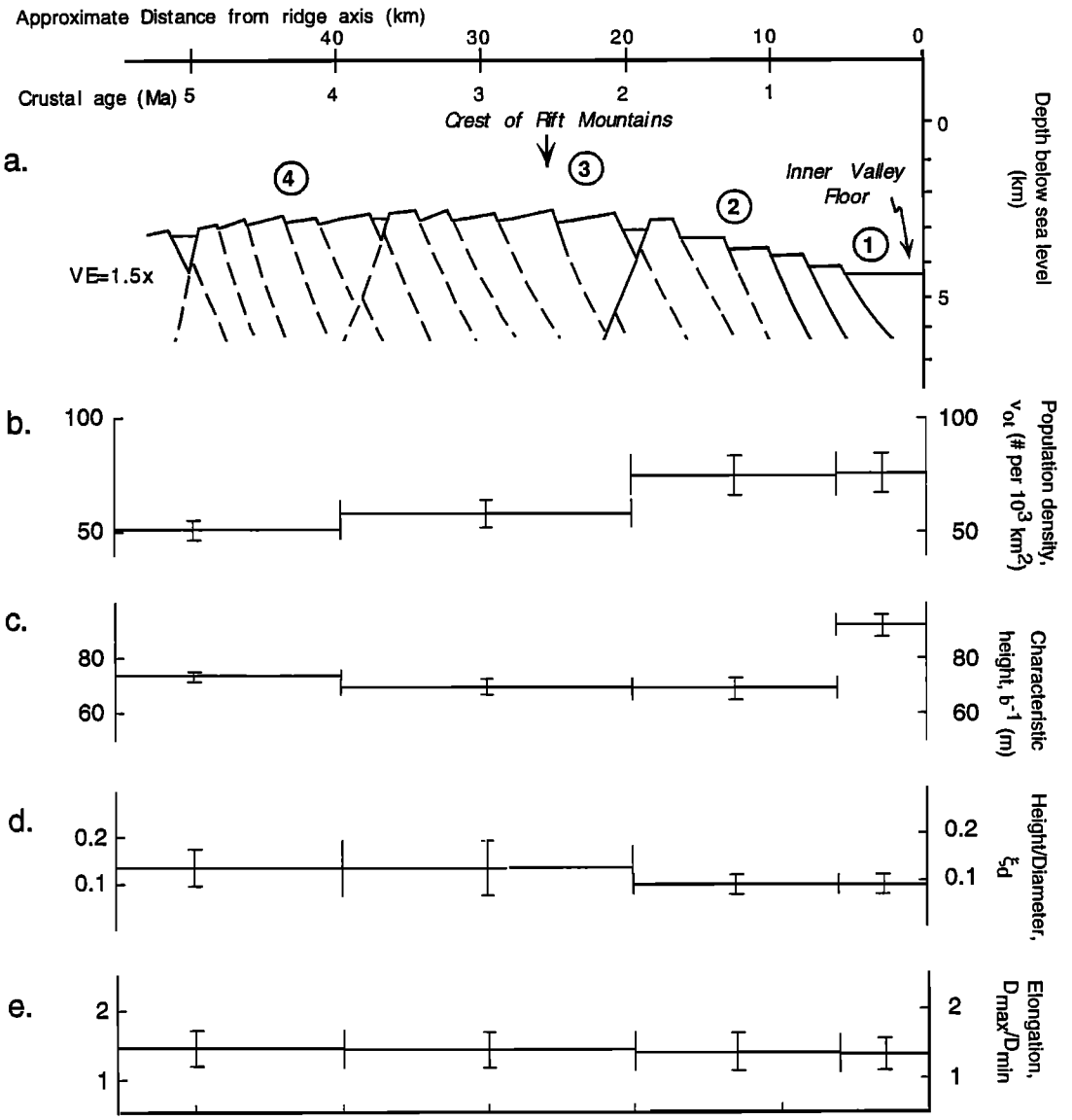

Figure 10. (a) Schematic cross-section showing presumed pattern of normal faulting [*Laughton and Searle*, 1979; G. Jaroslow and B. E. Tucholke, manuscript in preparation, 1999]. Inactive faults are indicated by dashed lines. Circled numbers identify (1) the relatively unfaulted inner rift valley floor, (2) the lower walls of the rift valley where faults are predominantly inward facing, (3) the upper rift valley wall to the crest of the rift mountains, where limited outward facing faults are active, and (4) ridge flank where there are no active faults. (b-e) Seamount population characteristics in age bins as indicated. Errors of one standard deviation are shown by vertical bars.

may be caused by any of several factors: (1) eruption along part of a fissure rather than at a restricted vent, (2) partial burial by subsequent, closely adjacent volcanism, (3) influence of preexisting topography, and (4) effects of minor, normal faulting. All these factors must be affected to some degree by extension in the spreading direction, although significant variability in seamount orientation ϕ shows that the effect is not strong (Figure 5).

6.1.2. 0.6-2 m.y. The first major modification of the seamount population occurs beyond the bounding fault in >0.6 Ma crust (Zone 2, Figure 10). We attribute this modification primarily to faulting. Studies of faults in the lower rift-valley walls [*Macdonald and Luyendyk*, 1977; *Jaroslow*, 1997; G. Jaroslow and B.E. Tucholke, manuscript in preparation, 1999] show that uplift occurs predominantly along normal, inward facing faults (faults *f*1, Figure 11). Inward jumping of the main bounding fault captures sections of the inner rift valley floor, with fault spacing of ~1-3 km [*Laughton and Searle*, 1979]. Basal diameters of observed axial seamounts also are mostly in the range of 1-3 km, so a significant proportion of seamounts is expected to be faulted. In the population studied here, we observe that ~30% of all off-axis seamounts are cut by inward facing faults.

A clear indication that the seamount population is affected by faulting beyond 0.6 Ma is the change in seamount orientations from widely varying on axis to a definitive trend that parallels the strike of normal faults on the ridge flank (Figure 5). We know of no other mechanism that would explain this reconfiguration.

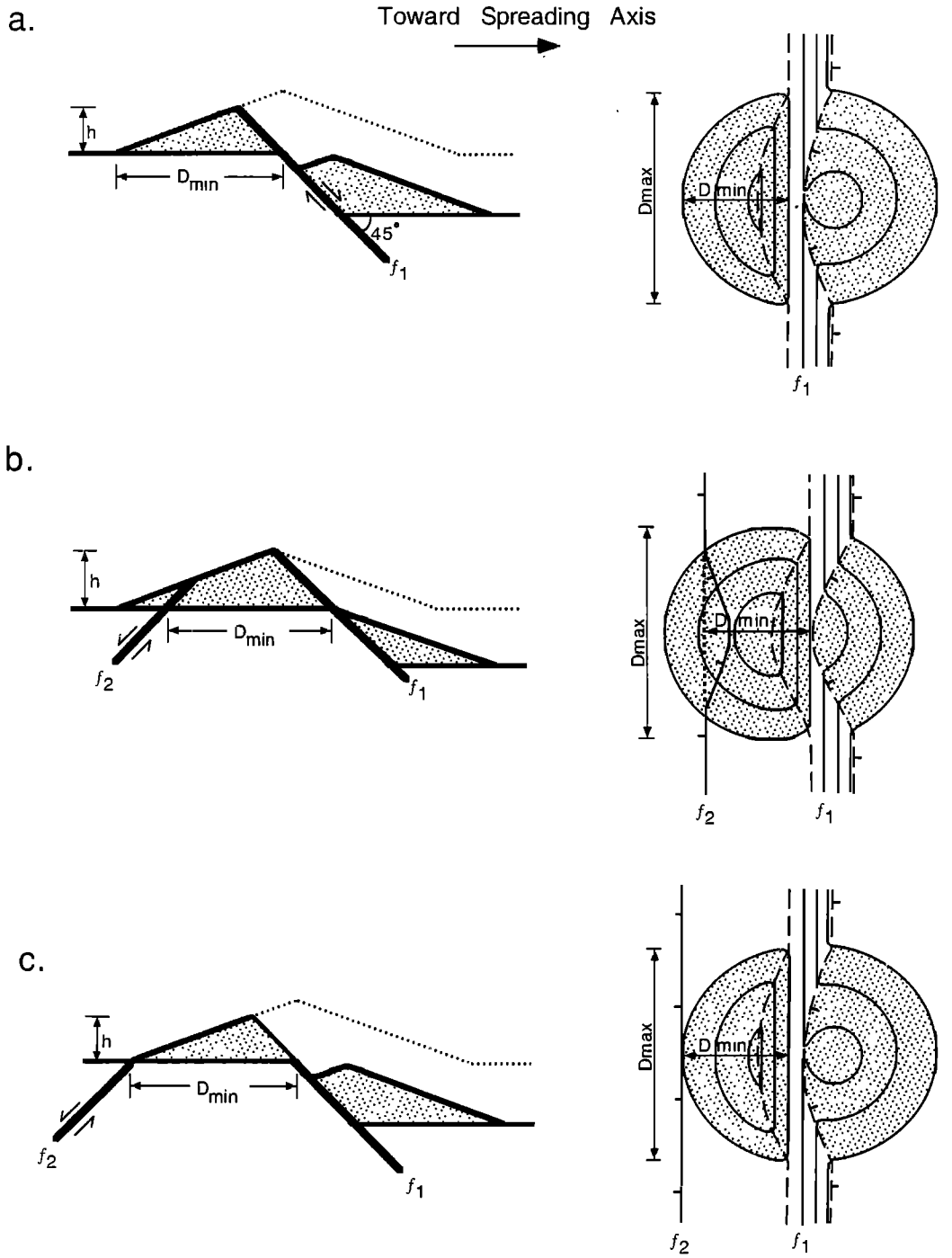

Figure 11. Illustrations showing effects of faults on seamount geometry (left) in cross section and (right) in corresponding plan view with schematic contours. Seamount volume above base level is stippled. Slopes of 20° on seamount flank and fault dips of 45° are assumed in this example. First generation, inward facing faults are designated as *f*1, and second generation, outward facing faults as *f*2. Active faults are indicated by arrows. Dashed lines in plan view show limits of exposed fault scarp. (a) Up to half of a seamount (at base level) can be downfaulted by *f*1 faults while maintaining $D_{max}/D_{min} \leq 2$ so that the seamount remains in the counted population. The downfaulted portion is rarely recognizable, probably because it is buried by talus and sediment at the base of the fault scarp. (b) Fault *f*1 intersects the crest of a seamount. At least for larger seamounts, this is probably the usual minimum extent of a seamount that is downfaulted; removal of a smaller portion does not reduce characteristic height, contrary to observation (see text). Fault *f*2 is shown at the most axisward position where D_{max}/D_{min} still is ≤2. (c) Fault *f*1 is as in the limiting case of Figure 11a. Here, fault *f*2 cannot cut into the seamount without increasing D_{max}/D_{min} to >2 and thus eliminating the seamount from the counted population.

The strong decrease in characteristic height of $\beta^{-1} = 92 \pm 4$ m to 69 ± 4 m between on-axis and 0.6-2 Ma crust (Figure 10c) probably is caused largely by faulting. Faults are likely to intersect larger seamounts and remove their crests (Figure 11a) more frequently than they intersect smaller seamounts, thus disproportionately reducing the height of large seamounts and causing a reduction in the characteristic height of the population (i.e., increasing the slope β^{-1} of the line in Figure 3). Few seamounts appear to be completely destroyed, however, as indicated by nearly constant population density (Figure 10b). The relatively constant population density does not negate the importance of faulting; normal faults could downthrow as much as half of a seamount (measured at base level) including the seamount crest without increasing the aspect ratio beyond 2 (the maximum permitted by our identification criteria) (Figure 11a).

Height-to-diameter ratio ξ_d also remains nearly constant from the axial seamounts to those on 0.6-2 Ma crust, implying that diameters are being reduced in approximate proportion to the reduction in height (Figure 10d). Hence faulting must typically remove a seamount crest (Figure 11a). This configuration may be expected if the fracture and fissure system that feeds magma to the AVR is a zone of weakness that localizes normal faults. The axisward edges of resulting fault blocks would carry dissected remnants of the AVR and seamounts, forming "volcanic lips" as have often been observed elsewhere along the MAR [*Macdonald and Luyendyk*, 1977; *Laughton and Searle*, 1979]. The effects of faulting also could be expected to appear in seamount elongation, D_{max}/D_{min}; there is no statistically significant change observed in the elongation parameter (Figure 10e), but because the error bars are large, this effect is not precluded.

Other factors might contribute to changes in seamount heights off-axis. The heights to which seamounts were initially constructed at the axis could have changed with time, but we consider it unlikely that the change in characteristic height represents a fundamental change in the nature of seamount accretion for two reasons. First, it would be remarkable that this change coincides with the boundary between the floor and wall of the rift valley, and second, the height change is 3 times that in any comparable time period over the preceding ~26 m.y. of crustal accretion (Figure 6). Mass wasting could also modify seamounts because it has been identified as a process that significantly affects both axial and off-axis crust [*Cann et al.*, 1992; *Allerton et al.*, 1995; *Tucholke et al.*, 1997b]. However, the observed reduction of seamount characteristic height would require height reduction of large seamounts by mass wasting in preference to small seamounts, and it is not clear how this could be accomplished. Significant mass wasting could also reduce population density by eliminating seamounts from our counting criteria (≥70 m height), but this is not observed. From these considerations we conclude that faulting is the major factor that affects the seamount population in the lower rift valley walls.

6.1.3. 2-4 m.y. Modification of the seamount population continues through the upper rift valley walls to the crest of the rift mountains (zone 3 at ~2-3 Ma, Figure 10; see also Figure 6). There is a significant reduction in seamount population density ν_α from 0.6-2 Ma to 2-4 Ma crust, while characteristic height, height-to-diameter ξ_d and elongation remain unchanged within their standard errors, although the range and mean of ξ_d do increase. These observations appear to be explained by a combination of sedimentation and mass wasting, with additional contributions by faulting and fault block rotation.

Reduction of population density in this region may be largely caused by sedimentation and mass wasting. Although average sediment cover on 2-4 Ma crust is low (8 m), several tens of meters of sediment can fill basement depressions between abyssal hills and near nontransforms offsets [*Jaroslow*, 1997]. Reduction in seamount height by sediment cover or by talus accumulation at the seamount base would reduce the counted seamount population as previously mentioned. Because these effects are likely to reduce heights of all seamounts uniformly, they will not change the slope of the population distribution and thus will not change the characteristic height (Figure 10c).

A small number of outward facing faults appear near the crest of the rift mountains [*Laughton and Searle*, 1979; G. Jaroslow and B. E. Tucholke, manuscript in preparation, 1999], and these faults also may modify the seamount population. Unlike earlier inward facing faults, however, an outward facing fault can only cut a small section of a previously faulted seamount without D_{max}/D_{min} exceeding 2 such that the seamount drops from the counted population (Figures 11b and 11c). The effects of outward facing faults that intersect seamounts consequently are to decrease seamount diameter in the counted population (thus increasing height-to-diameter ratio and elongation) and to reduce population density. Both reduced population density (Figure 10b) and increased range and mean of height-to-diameter ratio are observed (Figure 10d). Larger seamounts should be more affected by faulting, and this may account for increasing height–to-diameter ratio of larger seamounts in the 2-3 Ma and older age bins (Figure 7). Because the crests of previously faulted seamounts are now unlikely to be removed by outward facing faults without D_{max}/D_{min} exceeding 2 (Figures 11c and 11d), large seamounts are not disproportionately affected by faulting compared to small seamounts (as they were on 0.6-2 Ma crust), so the characteristic height is unchanged (Figure 10c). There is no statistically significant increase in elongation, but the large error bars on this parameter do not preclude increased elongation.

Tilting of fault blocks also could affect seamount shape, although it can not reduce the seamount population density (Figure 10b). Backtilt of blocks bounded by inward facing faults has been measured at 5°-10° [*Macdonald and Luyendyk*, 1977; *Laughton and Searle*, 1979] and, in some places, may reach 35°-40° [*Karson and Rona*, 1990]. We expect this backtilting to culminate at its highest value near the crest of the rift mountains before crust begins to subside on the ridge flank. The effect of any rotation would be to reduce plan view diameter in the flowline direction while effectively maintaining seamount height h and diameter in the along-isochron direction. The result would be an increase in height-to-diameter ratio and elongation, similar to the effects of faulting already discussed.

6.1.4. 4-28 m.y. There are few, if any, active faults on the ridge flank beyond the crest of the rift mountains [*Jaroslow*, 1997]. Therefore changes in seamount population characteristics on crust older than 4 Ma reflect either the effects of sedimentation and mass wasting or temporal changes in seamount production. Average sediment cover in the study area increases in thickness to a maximum of 35-50 m on 8-19 Ma crust and then decreases to 20-25 m on 19-28 Ma crust [*Jaroslow*, 1997]. As already noted, the effect of uniform partial burial of seamounts by sedimentation is to reduce the seamount population density without changing the characteristic height of the population. It is likely that the distribution of sediment cover accounts for much of the observed decline in seamount population density at 8-16

Ma and the increase at 16-24 Ma (Figure 6a). However, the peak in seamount abundance at 20-24 Ma is coeval with a major plate reorientation event [*Tucholke et al.*, 1997a] and we cannot discount the possibility that this event affected seamount production. The decline in seamount population density at 24-28 Ma is not a sedimentation effect and probably reflects a real decrease in seamount production.

Mass wasting of some seamounts is observed in scalloping of scarps and by decreased slope gradients characteristic of talus deposition at the seamount base. This has the effect of reducing population density with time, and it probably contributes to the long wavelength decrease in ν_α (Figure 6). However, as we have noted, mass wasting should have no effect on characteristic height. Thus the long-term trend of decreasing characteristic height with age (Figure 6b) is puzzling. If it is caused by a crustal aging process, it must preferentially reduce the height of larger seamounts in a way that we do not yet understand. It is possible that it reflects a real change in characteristic height of the original, axial seamount population over time, but the underlying mechanism is unknown.

6.2. Seamount Populations in Relation to Ridge Segmentation

Seamount population densities and characteristic heights do not change along isochrons (Table 4). There are not enough on-axis seamounts in our study area to be certain that this is true on the rift valley floor, but the fact that the observation is robust for off axis seamounts suggests that it also applies on axis. This is surprising because gravity studies [*Kuo and Forsyth*, 1988; *Lin et al.*, 1990] and seismic studies [*Tolstoy et al.*, 1993] suggest that crust is thickest near segment centers and therefore that magmatism might be strongest near segment centers.

At the bottom of the rift valley, the apparent along-axis uniformity of seamount abundance and characteristic height implies uniform eruption processes. This could be accomplished either by dike emplacement vertically from magma bodies that are evenly distributed along axis or by lateral magma propagation in dikes extending from a source at the segment center. Thus the uniform seamount population does not constrain whether deep-seated upwelling is focused near the segment center.

It is possible that seamount production actually is not uniform along axis but that we cannot detect variations from existing data. For example, seamount construction may be more frequent at segment centers than at segment ends, but segment center seamounts could be buried by subsequent volcanism, thus limiting the population density. This idea is consistent with overall along-axis topography and morphology of axial volcanic ridges in our study region; the AVR are robust near the segment center but tend to lose definition and become discontinuous toward the ends of segments.

It is also surprising that there is no difference in seamount population parameters between inside and outside corners of ridge segments off-axis (Table 4). IC crust is characteristically a region of highly strained thin crust (high RMBA) with irregular, large-throw normal faults and large detachment faults; the detachment faulting is thought to remove much of the volcanic crust from inside corners (footwalls) and transfer it to outside corners (hanging walls) [*Dick et al.*, 1981; *Karson*, 1990; *Tucholke and Lin*, 1994; *Escartín and Lin*, 1995]. Strain in OC crust also is less disruptive, with brittle extension being accommodated on relatively small-throw normal faults; apparent crustal thicknesses at OC remain comparable to those on axis [*Tucholke and Lin*, 1994; *Escartín and Lin*, 1995; *Jaroslow*, 1997]. From these observations we expect that seamount population densities would be lower at IC where more seamounts might be destroyed and higher at OC to which upper crust and seamounts would be transferred by detachment faulting. We do observe that seamount population densities are relatively low in regions of high RMBA and apparently thin crust (Table 3), but this observation does not hold for IC tectonic settings where RMBA is also generally elevated. It is possible that our artificial assignment of some percentage (30 or 14%) of segment length to "IC crust" explains this result; this assignment averages over cross-isochron variations in RMBA, and it may mask real correlations with seamount populations.

Significant differences in observed seamount populations between individual ridge segments (Table 2) suggest that seamount-forming volcanic processes are separate and distinct between segments. Differences in RMBA between segments within our study area, and also on the MAR at 29°-31°30'N [*Pariso et al.*, 1995], suggest there are no segment-to-segment correlations in magmatism. The trend of increasing seamount population densities and characteristic heights northward from segment E through segment H is noteworthy, and it is possible that the trend reflects increasing proximity to the Azores hotspot. However, off-axis seamount populations will have to be mapped farther to the north to determine whether the trend is a regional or local phenomenon.

7. Summary

The major conclusions of this study are the following.

1. Eighty-six axial and 1290 off-axis seamounts (circular to elliptical volcanoes) with height ≥ 70 m were identified on the western flank of the Mid-Atlantic Ridge between 25°25' and 27°10'N, extending from the inner rift valley floor westward ~450 km to ~29 Ma crust. Analysis of sidescan sonar images and bathymetry shows no evidence for construction of seamounts off axis, indicating that seamount construction occurs primarily on the inner rift valley floor in this region.

2. Abundance of off-axis seamounts shows that as seafloor is carried off axis through the rift valley wall to the ridge flank (> 4 Ma crust), crustal deformation is concentrated along discrete faults (spaced at ~1-3 km) and that the deformation is not pervasive. Nevertheless, significant changes in seamount population density, size distribution, and shape occur between ~0.6 and 3-4 Ma. During initial transport of seamounts out of the rift valley (0.6-2 m.y.), inward facing faults commonly intersect larger seamounts and thus reduce characteristic height of the population, although few seamounts are destroyed. In the upper portions of the rift valley (2-4 m.y.), sedimentation, mass wasting, additional faulting (outward facing), and backtilting of fault blocks reduce the seamount population density and increase the height-to-diameter ratio without affecting characteristic height.

3. Volcanic lips [*Macdonald and Luyendyk*, 1977; *Laughton and Searle*, 1979] are common features outside the inner rift valley floor and are composed of faulted seamounts and remnants of axial volcanic ridges perched at the elevated edges of fault blocks. This structural relationship indicates that major faults often nucleate through the axial volcanic ridge, as suggested by *Ballard and van Andel* [1977] from studies of the French-American Mid-Ocean Undersea Study (FAMOUS) region at 37°N on the MAR.

4. Beyond the crest of the rift mountains (>4 m.y.) faults are no longer active, and changes in the seamount population reflect long-term crustal aging processes as well as temporal changes in

seamount production at the ridge axis. Long-term changes in observed seamount population density are mostly explained by variations in sediment cover with crustal age. A short-term peak in population density on 20-24 Ma crust also is at least partly explained by variation in sediment cover, but strongly reduced population density on 24-28 Ma crust is not. The change in population density between these periods correlates in time with a significant change in plate motion ~24 – 22 Ma, and this event could have affected population density through changes in magmatism or tectonism (e.g., reduced faulting). A steady decline in characteristic height of the seamount population with crustal age cannot be attributed to crustal aging processes such as sedimentation or mass wasting, which should affect all seamount sizes equally. Either the decrease reflects real changes in how seamounts were constructed at the ridge axis, or some presently unknown aging process preferentially degrades the larger seamounts.

5. Seamount population density estimated for the entire off-axis seamount population has a positive correlation with crustal thickness as inferred from gravity data, suggesting that increased seamount production accompanies increased magma supply to the crust. However, intrasegment, along-isochron variations in seamount population characteristics do not appear to correlate with differences in RMBA that generally are associated with IC, SC, and OC tectonic settings. It is uncertain whether this effect is real or whether it is an artifact of averaging because of the way the tectonic settings were defined (i.e., as percentages of segment length, rather than as detailed, but subjectively interpreted, tectonic boundaries).

6. There are no discernable variations in measured seamount population density with along-axis position in the rift valleys of individual spreading segments. Assuming that this is not an artifact of the limited axial data set, there are two possible explanations: (1) Along-axis production of seamounts is uniform, in which case eruption processes also must be relatively uniform on axis. (2) Seamount production varies along the axis, but it is not possible to identify its topographic signature either because of complete or partial burial of existing seamounts by subsequent volcanism.

Acknowledgments. We thank S. Garland for help in developing the software for seamount identification, Tamara Osychny for help in data entry, and L. Dolby for assistance in map processing. We also thank J. Escartín, R. W. Girdler, D. Scheirer, and R. C. Searle for constructive comments. This research was supported by ONR grants N00014-93-1-1153 (AASERT), N00014-94-1-0319, N00014-94-1-0466, and N00014-90-J-1621. B. E. Tucholke was also supported by NSF grant OCE 95-03561. Contribution 10068 of Woods Hole Oceanographic Institution.

References

Allerton, S., B. J. Murton, R. C. Searle, and M. Jones, Extensional faulting and segmentation of the Mid-Atlantic Ridge north of the Kane Fracture Zone (24°00'N to 24°40'N), *Mar. Geophys. Res., 17*, 37-61, 1995.

Ballard, R. D., and T. H. van Andel, Morphology and tectonics of the inner rift valley at lat 36°50'N on the Mid-Atlantic Ridge, *Geol. Soc. Am. Bull., 88*, 507-530, 1977.

Ballard, R D., R. T. Holcomb, and T. H van Andel, The Galapagos Rift at 86°W: sheet flows, collapse pits and lava lakes of the rift valley, *J. Geophy. Res., 84*, 5407-5422, 1979.

Batiza, R., P. J. Fox, P. R. Vogt, S. C. Cande, N. R. Grindlay, W. G. Melson, and T. O'Hearn, Morphology, abundance, and chemistry of near-ridge seamounts in the vicinity of the Mid-Atlantic Ridge ~26°S, *J Geol., 97*, 209-220, 1989.

Blackman, D. K., J. R. Cann, B. Janssen, and D. K. Smith, Origin of extensional core complexes: evidence from the Mid-Atlantic Ridge at Atlantis fracture zone, *J. Geophys. Res., 103*, 21,315-21,333, 1998.

Blackman, D. K., and D. W. Forsyth, The effects of plate thickening on three-dimensional, passive flow of the mantle beneath mid-ocean ridges, in *Mantle Flow and Melt Generation at Mid-Ocean Ridges, Geophys. Monogr. Ser*, vol. 71, edited by J. Phipps Morgan, D. K. Blackman, and J. M. Sinton, pp. 311-326, AGU, Washington, D.C., 1992.

Bonatti, E., and C.G A. Harrison, Eruption styles of basalt in oceanic spreading ridges and seamounts: Effect of magma temperature and viscosity, *J Geophys. Res*, 93, 2967-2980, 1988.

Cann, J., D. K. Smith, M. E. Dougherty, J. Lin, B. Brooks, S. Spencer, C. J. MacLeod, E. McAllister, R. A. Pascoe, and J. A. Keeton, Major landslides in the MAR median valley, 25°-30°N: Their role in crustal construction and plutonic exposure (abstract), *Eos Trans AGU, 73*, Fall Meet. Suppl., 569, 1992.

Cann, J. R., D. K. Blackman, D. K. Smith, E. McAllister, B. Janssen, S. Mello, E. Avgerinos, A. Pascoe, and J. Escartín, Corrugated slip surfaces formed at North Atlantic ridge-transform intersections, *Nature*, 385, 329-332, 1997.

Dick, H. J. B., W. B. Bryan, and G. Thompson, Low-angle faulting and steady-state emplacement of plutonic rocks at ridge-transform intersections (abstract), *Eos Trans. AGU*, 62 (17), Fall Meet. Suppl., 406, 1981.

Epp, D., and N. C. Smoot, Distribution of seamounts in the North Atlantic, *Nature, 337*, 254-257, 1989.

Escartín, J., and J. Lin, Ridge offsets, normal faulting, and gravity anomalies of slow spreading ridges, *J. Geophys. Res., 100*, 6163-6177, 1995.

Fornari, D. J., R. Batiza, and M. A. Luckman, Seamount abundances and distribution near the East Pacific Rise 0°-24°N based on SeaBeam data, in *Seamounts, Islands, and Atolls, Geophys. Monogr. Ser.*, vol. 43, edited by B. H. Keating et al., 13-21, AGU, Washington, D.C., 1987.

Gente, P., R. A. Pockalny, C. Durand, C. Deplus, M. Maia, G. Ceuleneer, C. Mével, M. Cannat, and C. Laverne, Characteristics and evolution of the segmentation of the Mid-Atlantic ridge between 20°N and 24°N during the last 10 Myr, *Earth Planet. Sci. Lett., 129*, 55-71, 1995.

Head, J. W., L. Wilson, and D. K. Smith, Mid-ocean ridge eruptive vent morphology and substructure: Evidence for dike widths, eruption rates, and evolution of eruptions and axial volcanic ridges, *J. Geophys. Res., 101*, 28,265-28,280, 1996.

Jaroslow, G. E., The geological record of oceanic crustal accretion and tectonism at slow-spreading ridges, Ph.D. thesis, 210 pp, MIT/WHOI Joint Prog. in Oceanogr. and Eng, Woods Hole Oceanog. Inst., Woods Hole, Mass., 1997.

Jordan, T. H., W. Menard, and D. K. Smith, Density and size distribution of seamounts in the Eastern Pacific inferred from wide-beam sounding data, *J. Geophys. Res., 88*, 10,508-10,518, 1983.

Karson, J. A., Seafloor spreading on the Mid-Atlantic Ridge: Implications for the structure of ophiolites and oceanic lithosphere produced in slow-spreading environments. *Ophiolites· Oceanic Crustal Analogues*, edited by J. Malpas et al., pp. 547-555, Geol Surv. Dep., Nicosia, Cyprus, 1990.

Karson, J. A., and P. A. Rona, Block-tilting, transfer faults, and structural control of magmatic and hydrothermal processes in the TAG area, Mid-Atlantic Ridge 26°N, *Geol. Soc. Am. Bull., 102*, 1635-1645, 1990.

Kleinrock, M. C., and S. E. Humphris, Structural asymmetry of the TAG rift valley: Evidence from a near-bottom survey for episodic spreading, *Geophys Res. Lett., 23*, 3,439-3,442, 1996.

Kong, L., R. S. Detrick, P. J. Fox, L. A. Mayer, and W. B. F. Ryan, The morphology and tectonics of the MARK area from Sea Beam and Sea MARC I observations (Mid-Atlantic Ridge 23°N), *Mar. Geophys Res*, *10*, 59-90, 1988.

Kuo, B. Y., and D. W. Forsyth, Gravity anomalies of the ridge-transform system in the South Atlantic between 31° and 34.5°S: Upwelling centers and variations in crustal thickness, *Mar. Geophys. Res., 10*, 205-232, 1988.

Laughton, A. S., and R. C. Searle, Tectonic process on slow spreading ridges, *Deep Drilling Results in the Atlantic Ocean: Ocean Crust*, Maurice Ewing Ser., vol. 2, edited by M. Talwani, C. G. Harrison, and D.E. Hayes, pp. 15-32, AGU, Washington, D.C., 1979.

Lin, J., and J. Phipps Morgan, The spreading rate dependence of three-dimensional mid-ocean ridge gravity structure, *Geophys. Res. Lett., 19*, 13-16, 1992.

Lin, J., G. M. Purdy, H. Schouten, J.-C. Sempéré, and C. Zervas Evi-

dence from gravity data for focused magmatic accretion along the Mid-Atlantic Ridge, *Nature, 344*, 627-632, 1990.

Lin, J., B. E. Tucholke, and M. C. Kleinrock, Off-axis "boudin-shaped" gravity lows on the western flank of the Mid-Atlantic Ridge at 25°25' - 27°10'N: Evidence for long-term pulses in magmatic accretion in spreading segments (abstract), *Eos Trans. AGU*, 74 (16), Spring Meet. Suppl., 380, 1993.

Litvin, V. M., and M. V. Rudenko, Distribution of seamounts in the Atlantic, *Dokl. Acad. Sci. USSR, Earth Sci. Ser., Engl. Transl., 213*, 223-225, 1973.

Macdonald, K. C., and B. P. Luyendyk, Deep-tow studies of the structure of the Mid-Atlantic Ridge crest near lat 37°N, *Geol. Soc. Am. Bull., 88*, 621-636, 1977.

Mitchell, N. C., A model for attenuation of backscatter due to sediment accumulations and its application to determine sediment thicknesses with GLORIA sidescan sonar, *J. Geophys. Res., 98*, 22,477-22,493, 1993.

Morris, E., and R. S. Detrick, Three-dimensional analysis of gravity anomalies in the MARK area, Mid-Atlantic Ridge 23°N, *J. Geophys. Res., 96*, 4355-4366, 1991.

Pariso, J. E., J.-C. Sempéré, and C. Rommevaux, Temporal and spatial variations in crustal accretion along the Mid-Atlantic Ridge (29°-31°30'N) over the last 10 m.y.: Implications from a three-dimensional gravity study, *J. Geophys. Res., 100*, 17,781-17,794, 1995.

Purdy, G. M., J.-C. Sempéré, H. Schouten, D. L. Dubois, and R. Goldsmith, Bathymetry of the Mid-Atlantic Ridge, 24°-31° N: A map series, *Mar. Geophys. Res., 12*, 247-252, 1990.

Rona, P. A., R. N. Harbison, B. G. Bassinger, R. B. Scott, and A. J. Nalwalk, Tectonic fabric and hydrothermal activity of Mid-Atlantic Ridge crest (lat 26°N), *Geol. Soc. Am. Bull., 87*, 661-674, 1976.

Scheirer, D. S., and K. C. Macdonald, Near-axis seamounts on the flanks of the East Pacific Rise, 8°N to 17°N, *J. Geophys. Res., 100*, 2239-2259, 1995.

Sclater, J. G., and L. Wixon. The relationship between depth and age and heat flow and age in the western North Atlantic, *The Geology of North America,* vol. M, *The Western North Atlantic Region,* edited by P. R. Vogt and B. E. Tucholke, pp. 257-270, Geol. Soc. Am., Boulder, Colo., 1986.

Searle, R. C., Submarine central volcanoes on the Nazca plate: High resolution sonar observations, *Mar. Geol., 53*, 77-102, 1983.

Sempéré, J.-C., J. Lin, H. Brown, H. Schouten, and G. M. Purdy, Segmentation and morphotectonic variations along a slow-spreading center: The Mid-Atlantic Ridge (24°00'N-30°40'N), *Mar. Geophys. Res., 15*, 153-200, 1993.

Severinghaus, J., and K. C. Macdonald, High inside corners at ridge-transform intersections, *Mar. Geophys. Res., 9*, 353-367, 1988.

Shen, Y., D. W. Forsyth, D. S. Scheirer, and K. C. Macdonald, Two forms of volcanism: Implications for mantle flow and off-axis crustal production on the west flank of the southern East Pacific Rise, *J. Geophys. Res., 98*, 17,875-17,889, 1993.

Smith, D. K., and J. R. Cann, Hundreds of small volcanoes on the median valley floor of the Mid-Atlantic Ridge at 24-30°N, *Nature, 344*, 427-431, 1990.

Smith, D K , and J. R. Cann, The role of seamount volcanism in crustal construction at the Mid-Atlantic Ridge (24°-30°N), *J. Geophys. Res., 97*, 1645-1658, 1992.

Smith, D. K., and T. H. Jordan, Seamount statistics in the Pacific Ocean, *J. Geophys. Res., 93*, 2899-2918, 1988.

Smith, D. K., S. E. Humphris, and W. B. Bryan, A comparison of volcanic edifices at the Reykjanes Ridge and the Mid-Atlantic Ridge at 24°-30°N, *J. Geophys. Res , 100*, 22,485-22,498, 1995.

Temple, D. G., R. B. Scott, and P. A. Rona, Geology of a submarine hydrothermal field, Mid-Atlantic Ridge, 26°N latitude, *J. Geophys. Res., 84*, 7453-7466, 1979.

Tolstoy, M., A. J. Harding, and J. A. Orcutt, Crustal thickness on the Mid-Atlantic Ridge: Bull's-eye gravity anomalies and focused accretion, *Science, 262*, 726-729, 1993.

Tucholke, B. E., and J. Lin, A geological model for the structure of ridge segments in slow-spreading ocean crust, *J. Geophys. Res., 99*, 11937-11958, 1994.

Tucholke, B. E., J. Lin, and M. C. Kleinrock, Crustal structure of spreading segments on the western flank of the Mid-Atlantic ridge at 25°25'N to 27°10'N (abstract), *Eos Trans. AGU, 73*, Fall Meet. Suppl., 537-538, 1992.

Tucholke, B. E., J. Lin, M. C. Kleinrock, M. A. Tivey, T. B. Reed, J. Goff, and G. E. Jaroslow, Segmentation and crustal structure of the western Mid-Atlantic Ridge flank, 25°25' - 27°10'N and 0-29 m.y., *J. Geophys. Res., 102*, 10,203-10,223, 1997a.

Tucholke, B. E., W. K. Stewart, and M. C. Kleinrock, Long-term denudation of ocean crust in the central North Atlantic Ocean, *Geology, 25*, 171-174, 1997b.

White, S. M., K. C. Macdonald, D. S. Scheirer, and M.-H. Cormier, Distribution of isolated volcanoes on the flanks of the East Pacific Rise, 15.3°S-10°S, *J. Geophys. Res., 103*, 30,371-30,384, 1998.

Whitehead, J. A., H. J. B. Dick, and H. Schouten, A mechanism for magmatic accretion under spreading centers, *Nature, 312*, 146-148, 1984.

G. E. Jaroslow, Sea Education Association, P. O. Box 6, Woods Hole, MA 02543. (garyj@sea.edu)

D. K. Smith and B. E. Tucholke, Department of Geology and Geophysics, Woods Hole Oceanographic Institution, Woods Hole, MA 02543. (smith@humm.whoi.edu; btucholke@whoi.edu)

(Received October 1, 1998; revised June 4, 1999;
accepted July 14, 1999.)